J Appl Electrochem (2010) 40:457–461
DOI 10.1007/s10800-009-0016-y

ORIGINAL PAPER

The passivity of AISI 316L stainless steel in 0.05 M H_2SO_4

A. Fattah-alhosseini · A. Saatchi · M. A. Golozar · K. Raeissi

Received: 3 March 2009 / Accepted: 25 September 2009 / Published online: 8 October 2009

Abstract The passivity of AISI 316L stainless steel (AISI 316L) in 0.05 M H_2SO_4, in the steady-state condition, has been explored using various electrochemical techniques, including potentiostatic polarization, electrochemical impedance spectroscopy (EIS), and Mott–Schottky analysis. Based on the Mott–Schottky analysis in conjunction with the point defect model (PDM), it was shown that the calculated donor density decreases exponentially with increasing passive film formation potential. The thickness of the barrier layer was increased linearly with the film formation potential. These observations were consistent with the predictions of the PDM, noting that the point defects within the barrier layer of the passive film are metal interstitials, oxygen vacancies, or both. Also no evidence for *p*-type behavior was obtained, indicating that cation vacancies do not have any significant population density in the passive film.

Keywords PDM · Passive film · EIS · Formation potential · Stainless steel

1 Introduction

The passive films formed on stainless steels are known to exhibit semiconducting properties, because of their non-stoichiometric nature. Depending on the predominant defects present in the passive oxide layer on stainless steels, either *p*-type or *n*-type behaviors are observed. The passive oxide films with a deficiency in metal ions or excess with cation vacancies generally behave as *p*-type. Similarly, *n*-type is developed in the passive films either by excess cation in interstitial sites or anion vacancies. Mott–Schottky analysis has been shown to be an important in situ method for investigation of the semiconductor properties of passive films [1–5]. Compared with many theories describing the passive state qualitatively, the PDM [6–10] provides a microscopic description of the growth and breakdown of the passive film, as well as an analytical expression for the flux and concentration of vacancies within the passive film. Therefore this model can also provide an opportunity for quantitative analysis of the passive film. The PDM is based on the migration of point defects under the influence of electrostatic field within the passive film. Because the passive film grows into the metal by the generation of oxygen vacancies at the metal/passive film interface, and by their annihilation at the passive film/solution interface, the transport properties and spatial distribution of oxygen vacancies or metal cations within the passive film are of the great interest.

A key parameter in describing the transport of point defects and hence the kinetics of passive film growth is the diffusivity of the point defects. Inspite of relatively extensive works published on the passive films, there seems to be lack of study on the density and diffusivity of point defects in the passive films formed on stainless steels in acidic solutions. In this work, EIS and Mott–Schottky analysis of AISI 316L have been performed. The ultimate goal of this study is to model experimental data within the PDM. This work includes determination of the passive region for AISI 316L in 0.05 M H_2SO_4, measurement of steady-state current for the region of passive film formation, determination of the semiconductor character, and estimation of the dopant levels in the passive film, as well

A. Fattah-alhosseini (✉) · A. Saatchi · M. A. Golozar · K. Raeissi
Department of Materials Engineering, Isfahan University of Technology, Isfahan 84156-83111, Iran
e-mail: arash.fattah@Gmail.com

as the estimation of the film thickness as a function of the formation potential.

2 Experimental procedures

Specimens were fabricated from 1 cm diameter rods of AISI 316L with the chemical composition (wt%): Cr 17.5, Ni 13.4, Mo 2.32, Mn 1.4, Si 0.47, C 0.04, S 0.003, and balance Fe. The samples were placed in stainless steel sacks and annealed in inert environment (Ar gas) to eliminate the cold work effect due to cutting process. The annealing was preformed at 1050 °C for 90 min followed by water quenching. All samples were ground to 1200 grit and cleaned by ethanol and deionized water prior to tests. A three-electrode cell featuring a Pt counter electrode and a saturated calomel electrode (SCE) was employed. All the potential values in the text are relative to the SCE. The solution (0.05 M H_2SO_4) was prepared from analytical grade 97% H_2SO_4 and distilled water. Before potentiostatic film growth, the electrode was held at −1.2 V for 5 min to remove the native oxide film.

All electrochemical measurements were obtained using a PARSTAT 2273 advanced electrochemical system at ambient temperature (23–25 °C). A polarization curve was obtained at a potential scan rate of 1 mV/s. Four potentials within the passive region were chosen for potentiostatic film growth and EIS measurements, 0, 0.2, 0.4, and 0.6 V. Films were gown at each potential for 1 h to insure that the system was in steady-state. After each film growth period, EIS measurements were performed. The frequency was scanned between 0.01 Hz and 100 kHz and with an excitation potential of 10 mV (peak-to-peak). Mott–Schottky experiments were done by measuring the frequency response at 1 kHz during a 25 mV/s negative potential scan from 0.6 to 0.0 V.

3 Results and discussion

3.1 Polarization measurement

Figure 1 shows the potentiodynamic curve for the AISI 316L electrode in 0.05 M H_2SO_4. From the polarization curve, the passive range was determined to be from −0.1 to 0.7 V. It was observed that before the electrode was transferred to a passive state an active current peak occurred at around −0.15 V, which could be attributed to the oxidation of Fe^{2+} to Fe^{3+} ions in the passive film [11, 12].

During the formation of the oxide films on working electrode, the evolution of the current density measured during the application of different potentials (0, 0.2, 0.4, and 0.6 V) in the passive domain was recorded. Figure 2a displays the potentiostatic polarization curves for the AISI 316L in 0.05 M H_2SO_4 at selected formation potentials. It was observed that the current density diminishes with time

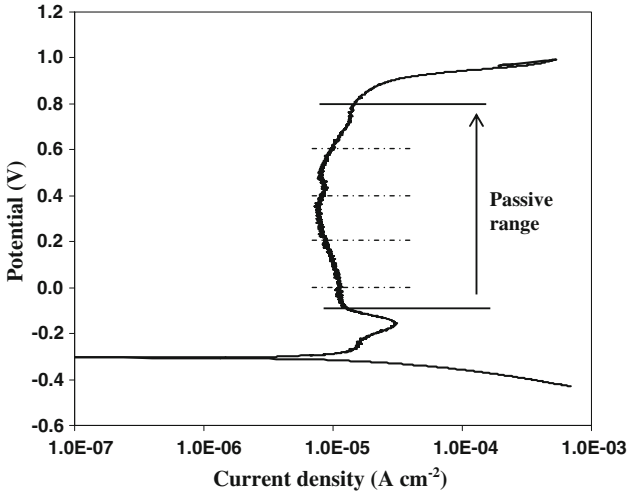

Fig. 1 Polarization curve of AISI 316L in 0.05 M H_2SO_4 in the anodic direction at 1 mV/s

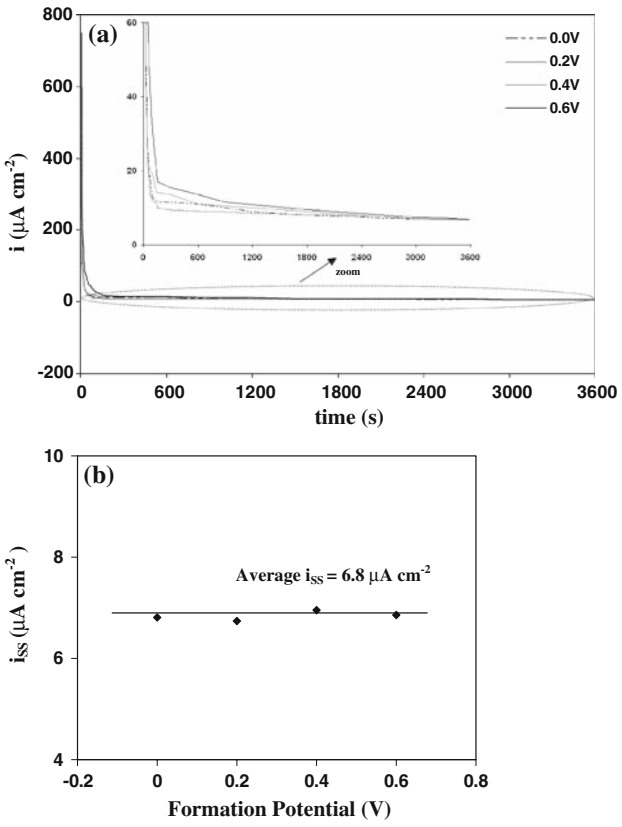

Fig. 2 **a** Potentiostatic polarization curves of AISI 316L in 0.05 M H_2SO_4, and **b** Steady-state passive current density obtained during the potentiostatic growth of the passive films; at different film formation potentials for 1 h

until a constant value is reached and a steady-state is established. Figure 2b shows the values of the steady-state passive current density (i_{ss}) versus the formation potential. The steady-state current density is approximately 6.8 μA cm^{-2}.

3.2 EIS measurements

The impedance spectra were measured at selected potentials in the passive film formation region. Nyquist plots, in which the imaginary component of the impedance is plotted against the real component as a function of frequency, are shown in Fig. 3. As predicted by PDM, the complex plane plot in the low frequency region is a straight line and is insensitive to the formation potential. The constant phase nature of the impedance at low frequencies is a consequence of defect transport in the oxide film being mainly due to migration under the influence of the electric field. The lack of sensitivity of the impedance locus to the applied formation potential is a manifestation of the electric field strength in the barrier layer being insensitive to the applied potential, which is one of the fundamental postulates underlying the PDM [13]. This ensures that the driving force for the transport of defects across the barrier layer is independent of the applied potential. Physically, the constant, field strength independent from applied potential is attributed to the buffering effect of Esaki (band-to-band) tunneling of electrons and holes in the barrier layer [13–15].

3.3 Mott–Schottky analysis

Mott–Schottky analysis has been employed to determine the semiconductor type and dopant density of the passive film. The equations for Mott–Schottky analysis are [13, 16]:

$$\frac{1}{C_{SC}^2}=\frac{2}{\varepsilon\varepsilon_0 eN_D}\left(E-E_{FB}-\frac{k_BT}{q}\right) \quad \text{for n-type semiconductor} \tag{1}$$

$$\frac{1}{C_{SC}^2}=-\frac{2}{\varepsilon\varepsilon_0 eN_A}\left(E-E_{FB}-\frac{k_BT}{q}\right) \quad \text{for p-type semiconductor} \tag{2}$$

where ε is the electron charge, N_D and N_A are the donor and acceptor density (cm^{-3}), ε is the dielectric constant of the passive film ($\varepsilon = 12$ [13, 17–19]), ε_0 is the vacuum permittivity (8.854×10^{-14} F/cm), K_B is the Boltzmann constant (1.38×10^{-23} J/K), T is the absolute temperature, and E_{FB} is the flat band potential. The interfacial capacitance, C, is obtained from [15]:

$$C=-\frac{1}{\omega Z_{img}} \tag{3}$$

where Z_{img} is the imaginary component of the impedance and $\omega = 2\pi f$ is the angular frequency. Assuming that the capacitance of the double layer can be neglected, the measured capacitance C is equal to the space charge capacitance, C_{SC}. Neglecting the double layer capacitance requires that the space charge capacitance be at least 1–2 orders lower than the specific double layer capacitance and must be significantly higher than the parallel geometric capacitance for this assumption to be valid [18, 20].

Figure 4 represents C^{-2} versus potential plots for a passive film formed on AISI 316L in 0.05 M H_2SO_4 at selected formation potentials. Figure 4 displays positive slopes, indicative that *n*-type semiconductor behavior exists at all formation potentials. From the linear part of the

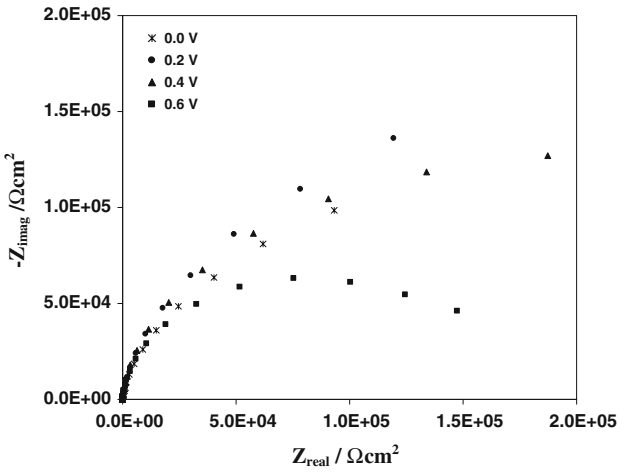

Fig. 3 Nyquist plot for AISI 316L in 0.05 M H_2SO_4 measured at different film formation potential

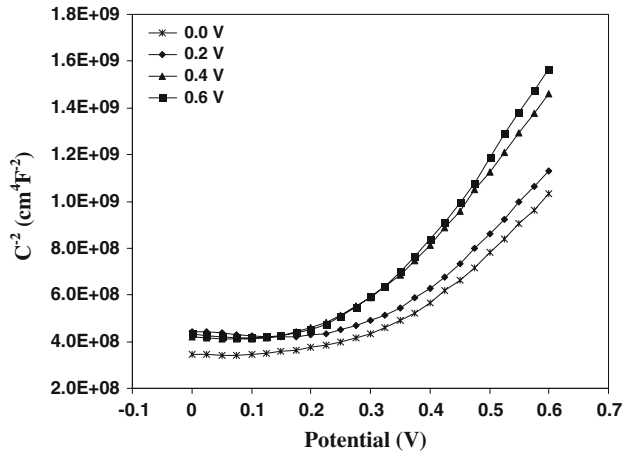

Fig. 4 Mott–Schottky plots of C^{-2} as a function of potential for passive films on AISI 316L formed at the potentials of 0, 0.2, 0.4, and 0.6 V in 0.05 M H_2SO_4

slopes a donor density can be estimated. The dopant density calculated with this method indicates the density close to the alloy/passive film interface, where the concentrations of oxygen vacancies and metal interstitials are predicted to be the highest.

Figure 5 displays the donor density as a function of the formation potential. Similar values for the donor density have been observed, and the tendency of the donor density to decrease with increasing potential has been reported by Sikora and Macdonald [1, 6, 21]. Other studies have shown that the relationship between donor density and the formation potential can be developed theoretically on the basis of the PDM [21–23].

According to the PDM, the flux of oxygen vacancy through the passive film is essential to the film growth process, which supports the existence of oxygen vacancy in the film regardless of its concentration. In this concept, the dominant point defects in the passive film are considered to be oxygen vacancies and/or cation interstitials acting as electron donors. However, as it is impossible to separate the contribution of oxygen vacancies and cation interstitials on the measured diffusivity value based on the PDM, the diffusivity is considered to be dependent on the combination effects of these two-point defects [24].

This theoretical relationship yields a good fit to the experimental results, and allows the diffusivity of defects in the passive film to be calculated. The relevant equation describing the dependency of the donor density on the formation potential is shown as Eq. 4, where ω_1, ω_2, and b are unknown constants that are to be determined from the experimental data [21, 22]:

$$N_{\mathrm{D}} = \omega_1 \exp(bE) + \omega_2 \tag{4}$$

Based on the nonlinear fitting of the experimental data by the software, the exponential relationship between the donor density and the formation potential is derived as:

$$N_{\mathrm{D}} = 0.9658 \times 10^{21} \exp(-5.1021E) + 2.4782 \times 10^{21} (\mathrm{cm}^{-3}) \tag{5}$$

The diffusion coefficient can be calculated from Eq. 6 as follows [21, 22]:

$$D_0 = \frac{J_0}{2K\omega_2} = \frac{J_0 RT}{2F\omega_2 k} \tag{6}$$

$$J_0 = -\frac{i_{\mathrm{ss}}}{2e} \tag{7}$$

where $K = \frac{kF}{RT}$, k represents the electric field strength of the passive film, and i_{ss} is determined from the Fig. 2. The k was determined to be approximately 1.02×10^6 V/cm by Smialowska and Kozlowski [24] for the passive film grown on iron. Therefore, it is assumed that the value of k for the passive film on AISI 316L in 0.05 M H_2SO_4 to be approximately 10^6 V/cm. Substitution of i_{ss} (6.8×10^{-6} A cm^{-2}), e (-1.602×10^{-19} C), k (10^6 V/cm), ω_2 (2.4782×10^{21} cm^{-3}), R (8.314 J/mol K), T (298 K), and F (96500 C mol/e) into Eqs. 6 and 7 yields $D_0 = 1.1 \times 10^{-17}$ cm^2/s. Taking into account the error caused by the assumption of k in Eq. 6, the diffusion coefficient of defects in the passive film formed on AISI 316L in 0.05 M H_2SO_4 is estimated to be in the range of 10^{-17}–10^{-16} cm^2/s, which is in the order of the results reported for diffusion coefficient of defects in the passive film on carbon steel in borate solution at room temperature [25, 26].

Figure 6 shows a linear relationship between the steady-state film thickness (L_{ss}) and the formation potential. This relationship between the steady-state film thickness and the formation potential has been reported by Macdonald et al. [8–10, 13]. The film thickness was calculated from the capacitance measured at 1 kHz after each 1 h constant potential growth. It is assumed that, at this frequency, the electrochemical impedance is largely capacitive in nature,

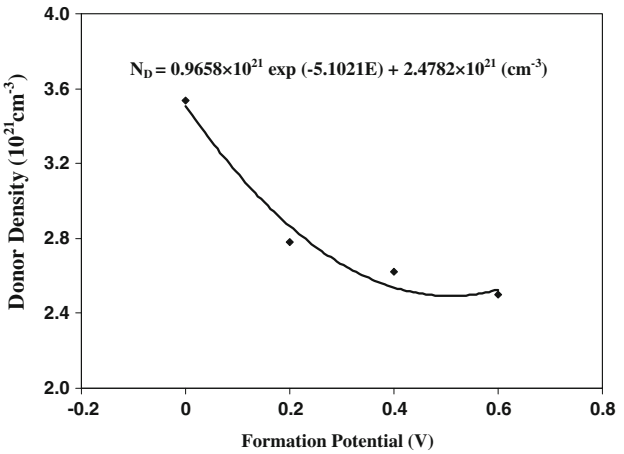

Fig. 5 Donor densities of the passive films formed on AISI 316L in 0.05 M H_2SO_4 as a function of film formation potential

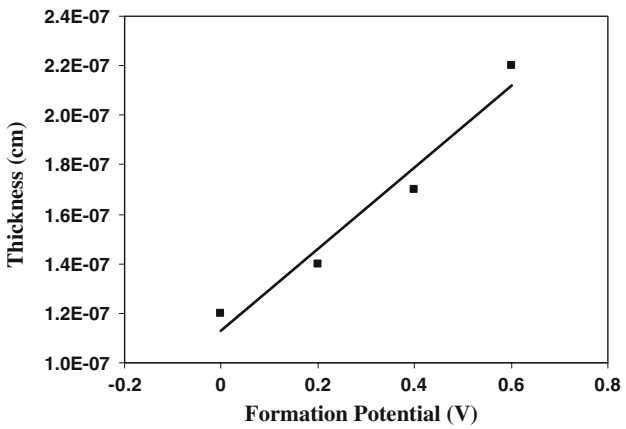

Fig. 6 Film thickness as a function of the formation potential. Thickness was measured after each 1 h film growth

with the measured capacitance being almost independent of frequency. The parallel plate expression was used for calculating the steady-state film thickness from the measured capacitance [1, 21]:

$$L_{ss} = \frac{\varepsilon\varepsilon_0}{C} \tag{8}$$

The calculated thickness ranges from about 1.3 nm at 0.0 V to 2.2 nm at 0.6 V. These values of the thickness are considered to be eminently realistic [8–10, 13, 27].

According to the PDM, the steady-state passive current density may be used to calculate the general corrosion rate using the formula [13]:

$$\frac{dL}{dt} = \frac{\bar{M}}{\bar{z}F\rho} i_{ss} \tag{9}$$

where $\bar{M}$ and $\bar{z}$ are the composition-averaged atomic weight and oxidation number, respectively and ρ is the density of the steel. Noting that

$$\bar{M} = \chi_{Fe}M_{Fe} + \chi_{Cr}M_{Cr} + \chi_{Ni}M_{Ni} + \chi_{Mo}M_{Mo} \tag{10}$$

and

$$\bar{z} = \chi_{Fe}z_{Fe} + \chi_{Cr}z_{Cr} + \chi_{Ni}z_{Ni} + \chi_{Mo}z_{Mo} \tag{11}$$

where χ_i is the atomic fraction, M_i is the atomic weight, and z_i is the oxidation number of element i in the steel, then the rate of penetration of general corrosion is readily calculated [13]. Thus, taking a generic AISI 316L as having a composition of 66.78 wt% Fe, 17.5 wt% Cr, 13.4 wt% Ni, and 2.32 wt% Mo, it is obtained that χ_{Fe}, χ_{Cr}, χ_{Ni}, χ_{Mo} are 0.6699, 0.1885, 0.1275, 0.0134, respectively. The composition-averaged atomic weight of the steel, as calculated from Eq. 10, is 56.125 g. Likewise, noting that z_{Fe}, z_{Cr}, z_{Ni}, and z_{Mo} are 2, 3, 2, and 6, respectively, the composition-averaged oxidation number is found from Eq. 11 to be 2.2407. Taking the density of AISI 316L as 7.99 g/cm^3, the corrosion rate calculated from Eq. 9 corresponding to a steady-state passive current density of 10^{-6} A/cm^2 (Fig. 2) is 3.248×10^{-11} cm/s or 10.242 μm/year. This corresponds to approximately 1 mm corrosion penetration in 100 years service.

4 Conclusions

Potentiodynamic polarization studies demonstrate that AISI 316L displays a wide passive range in 0.05 M H_2SO_4 at ambient temperature. Potentiostatic polarization tests revealed that the steady-state current density through the passive film formed on AISI 316L for 1 h was independent of formation potential, which is well consistent with the postulation of the PDM. Based on the Mott–Schottky analysis, it was shown that the calculated donor density decreases exponentially with increasing formation potential and the thickness of the barrier layer increases linearly with the formation potential. The experimental data were interpreted in terms of the PDM for the passivity of AISI 316L in 0.05 M H_2SO_4, assuming that the donors are defects including oxygen vacancies and cation interstitials. The calculated diffusivity of defect was in the range of 10^{-17}–10^{-16} cm^2/s.

References

1. Sikora E, Macdonald DD (1997) Solid State Ionics 94:141
2. Sikora J, Sikora E, Macdonald DD (2000) Electrochim Acta 45:1875
3. Cho EA, Kwon HS, Macdonald DD (2002) Electrochim Acta 47:1661
4. Hakiki NE, Montemor MF, Ferreira MGS, Da Cunha Belo M (2000) Corros Sci 42:687
5. Stimming U (1986) Electrochim Acta 31:415
6. Macdonald DD (1999) Pure Appl Chem 71:951
7. Macdonald DD (2004) Curr Appl Phys 4:129
8. Macdonald DD, Sun A (2006) Electrochim Acta 51:1767
9. Macdonald DD (2008) J Nucl Mater 37:924
10. Macdonald DD (2006) J Electrochem Soc 153:B213
11. Azumi K, Ohtsuka T, Sata N (1987) J Electrochem Soc 134:1352
12. Macdonald DD, Ismail KM, Sikora E (1998) J Electrochem Soc 145:3141
13. Nicic I, Macdonald DD (2008) J Nucl Mater 379:54
14. Macdonald DD, Smedley SI (1990) Electrochim Acta 35:1949
15. Sikora E, Macdonald DD (2002) Electrochim Acta 48:69
16. Di Paola A (1989) Electrochim Acta 34:203
17. Hakiki NE, Da Cunha Belo M, Simoes AMP, Ferreira MGS (1998) J Electrochem Soc 145:3821
18. Gaben F, Vuillemin B, Oltra R (2004) J Electrochem Soc 151:B595
19. Goodlet G, Faty S, Cardoso S, Freitas PP, Simoes AMP, Ferreira MGS, Da Cunha Belo M (2004) Corros Sci 46:1479
20. Raja KS, Jones DA (2006) Corros Sci 48:1623
21. Sikora E, Sikora J, Macdonald DD (1996) Electrochim Acta 41:783
22. Ahn SJ, Kwon HS (2004) Electrochim Acta 41:3347
23. Liu J, Macdonald DD (2001) J Electrochem Soc 148:B425
24. Smialowska SZ, Kozlowski W (1983) Passivity of metals and semiconductors, Netherlands
25. Cheng YF, Yang C, Luo JL (2002) Thin Solid Films 416:169
26. Bojinov M, Laitinen T, Makela K, Saario T (2001) J Electrochem Soc 148:B243
27. Olsson COA, Landolt D (2003) Electrochim Acta 48:1093